buildings

MDPI

Article

Behavior of Stiffened Rafts Resting on Expansive Soil and Subjected to Column Loads of Lightweight-Reinforced Concrete Structures

Mohamed H. Abu-Ali [1,*], Basuony El-Garhy [1], Ahmed Boraey [1], Wael S. Alrashed [1], Mostafa El-Shami [2], Hassan Abdel-Daiem [3] and Badrelden Alrefahi [1]

[1] Department of Civil Engineering, University of Tabuk, P.O. Box 741, Tabuk 71491, Saudi Arabia; belgarhy@ut.edu.sa (B.E.-G.); a.boraey@ut.edu.sa (A.B.); walrashed@ut.edu.sa (W.S.A.)
[2] Department of Civil Engineering, Faculty of Engineering, Menoufia University, Shibin El-Kom 32511, Egypt; mostafa.el-shami@protonmail.com
[3] Department of Electrical Engineering, University of Tabuk, P.O. Box 741, Tabuk 71491, Saudi Arabia; habdaldaiem@ut.edu.sa
* Correspondence: mabuali@ut.edu.sa

Abstract: An approach to estimate the behavior of stiffened rafts under column loads of a lightweight-reinforced concrete structure resting on expansive soils is presented in this paper. The analysis was conducted using the computer program SLAB97, which estimates the 3D distorted mound shape using the finite difference method by solving the transient suction diffusion equation in 3D and computing the corresponding soil movements. The interaction between the stiffened rafts and the 3D distorted mound shape is then analyzed using the finite element method. The SLAB97 program has been validated by comparing its results with the results of others that were shown to be valid. The goal of the study is to make the expansive soil structure interaction models that the previous researchers proposed more logical. Assuming the worst initial 3D distorted mound shapes of the two cases of edge heave and edge shrinkage, an upper-bound solution is obtained. Using the two scenarios of edge shrinkage and edge heave, the program was utilized in a parametric investigation to examine the impact of various parameters on the behavior of stiffened rafts on expansive soils. These parameters include the stiffening beam depth, the maximum differential movement of the distortion mound shape, and the raft dimensions. The behavior of the stiffened rafts subjected to concentrated column loads is concluded to be similar to that of the stiffened rafts subjected to uniform and perimeter line loads in both cases of distortion modes, with regard to the shape of raft deformation and distribution of the bending moments; however, the values of the design parameters such as maximum deflection, maximum differential deflection, and maximum moments are entirely different in these two situations.

Keywords: stiffened rafts; expansive soils; suction diffusion equation; lightweight-reinforced concrete structure; edge shrinkage; edge heave; distorted mound shape

Citation: Abu-Ali, M.H.; El-Garhy, B.; Boraey, A.; Alrashed, W.S.; El-Shami, M.; Abdel-Daiem, H.; Alrefahi, B. Behavior of Stiffened Rafts Resting on Expansive Soil and Subjected to Column Loads of Lightweight-Reinforced Concrete Structures. *Buildings* **2024**, *14*, 588. https://doi.org/10.3390/buildings14030588

Academic Editors: Zechuan Yu and Dongming Li

Received: 13 January 2024
Revised: 12 February 2024
Accepted: 18 February 2024
Published: 22 February 2024

1. Introduction

As is well known, the unsaturated expansive soils undergo movements (shrinkage or heave) in response to the changes in their moisture content (i.e., soil suction). The soil heaves and shrinks as its moisture content increases and decreases. The shrinkage or heave in expansive soils causes distortions in structures constructed over them, especially lightweight structures such as low to medium-rise buildings, commercial buildings, schools, hospitals, mosques, swimming pools, and rigid and flexible pavements. The changes in the soil suction may be caused by rainfall and evaporation, lawn irrigation, leaking from water or sewage pipelines, large trees, and raising or lowering in the groundwater table.

Lightweight structures constructed on expansive soils are frequently subjected to severe movements (shrink or heave) arising from non-uniform soil moisture changes,

with consequent cracking and damage related to the distortion. The damage caused by expansive soils can range from minor cracking in walls and sidewalks to major cracking in the structural elements of the structures. Damage to lightweight structures constructed on expansive soils has been widely reported in many countries of the world [1,2]. In the United States alone, the annual loss due to structural damage caused by expansive soils exceeds that caused by earthquakes, hurricanes, and floods combined [3]. According to Krohn and Slosson [4], the annual cost of expansive soil damage in the United States exceeded $7.0 billion. In Australia, expansive soils cause structural cracks in nearly 50,000 houses each year [5]. According to Dafalla et al. [6], Saudi Arabia's expansive soils are believed to have caused economic losses in the hundreds of millions of US dollars.

Expansive soil is found in many parts of the world; however, the problems usually appear in the areas of semi-arid, arid, and severely arid climates such as Egypt and Saudi Arabia [7,8]. Only 41 years ago, Erol and Dhowian [9] conducted research on the swell and shrinkage behavior of active Madinash clays, which led to the discovery of expansive soil in Saudi Arabia. For the long-term monitoring of changes in soil suction and the consequent volume changes (shrink/heave) in expansive soil, Dhowian et al. [10] set up a primary field station in Al-Ghatt town in Saudi Arabia. Ruwaih [11] and Abduljauwad et al. [12] revealed the sites in Saudi Arabia where expansive soils have been discovered. Since there has been a growth in urban development in Saudi Arabia since 1998, it is expected that the expansive soils will be discovered in other areas of the country. For this reason, it is crucial for researchers and civil engineers to update the extensive soil presence places in Saudi Arabia.

Several scholars (e.g., [13–18]) have reported on the features of the expansive soils in various parts of KSA. Sabtan [19] and Dafalla and Al-Shamrani [18] reported the subsurface conditions and the geotechnical properties of the expansive soils in Tabuk City. Abduljauwad [16] reported the swelling properties of the expansive soils for different locations in the Eastern Province of Saudi Arabia. Abduljauwad and Ahmed [14] reported case histories in the Eastern Province of Saudi Arabia, including the residential district north of AI-Mubarraz city in the AI Hassa area and the A1-Qatif housing project.

The types of damage observed in structures constructed on expansive soils in Saudia Arabia include serious cracks, tilting, twisting, and sticking doors and windows [15,20]. The authors observed damage in a number of private and government lightweight structures in the Al Masif district of Tabuk City. Examples of the observed damage are shown in Figure 1. These cracks occurred shortly after the initial use of the structures as a result of moisture migration into the expansive soils.

Soil movements and improper foundation system selection and design are the causes of these cracks. Nelson et al. [2] state that grade beams on drilled piers, stiffened strip footing, and stiffened rafts are foundation systems that have been used successfully with expansive soils.

The performance and construction cost of lightweight structures built on expansive soil are influenced by the choice of foundation system, and the determination and categorization of the expansive soil, as well as the superstructure loads, are necessary factors for the proper foundation system selection [21]. Nelson et al. [2] reported the variables that affect how structures are designed on expansive soils, as well as the design options available to builders: (1) building the structure to withstand expansion-related movements and/or swell pressures; (2) treating the expansive soil or managing the supporting soil's environment by taking preventative measures to reduce the movements; (3) combining the two options.

Designing the structure to be stiff enough to accommodate soil movements is one way to reduce damage for structures built on expansive soil [2,22,23]. Stiffened rafts and strip footings and inverted T sections are the two foundation systems that are successfully used in various countries around the world (i.e., United States, Australia, South Africa, Saudia Arabia, and Egypt) to reduce or eliminate the damage of lightweight structures constructed on expansive soils [2,21,23–25]. Given Saudi Arabia's Vision-2030, urbanization is growing quickly, which makes it more likely that lightweight structures can be built on expansive

soils in various parts of the country. This demonstrates the critical need for useful advice to assist civil engineers in minimizing or removing potential issues and damage to lightweight structures built on expansive soils, thereby lowering the loss of millions of dollars.

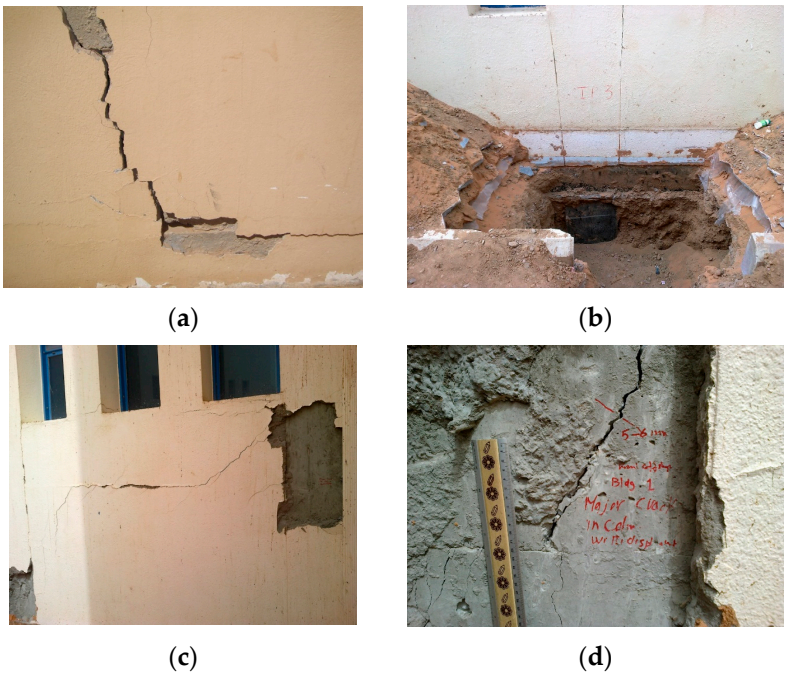

Figure 1. Examples of damage in lightweight structures constructed on expansive soils: (**a**) Cracks in a wall (Private building in Al Masif, Tabuk, Saudia Arabia), (**b**) Cracks in a ground beam (Government building in Al Masif, Tabuk, Saudia Arabia), (**c**) Cracks in a wall (Government building in Al Masif, Tabuk, Saudia Arabia), (**d**) Cracks in a column (Government building in Al Masif, Tabuk, Saudia Arabia).

Two primary items are presented in this study: Using the two scenarios of edge shrinkage, ES, and edge heave, EH, the program was utilized in a parametric investigation to examine the effect of various parameters on the behavior of stiffened rafts on expansive soils. Some of these parameters include the stiffening beam depth, the raft dimensions, and the mound shape's maximum differential movement. The three-story lightweight structure is made of reinforced concrete, which includes slabs, beams, columns, and a stiffened raft.

2. Analysis Method

2.1. Limitations in Existing Design Methods

Many design approaches have been documented and discussed in the literature for the design of a stiffened raft resting on expansive soils (e.g., [23,25–31]). Every one of the current design approaches has certain shortcomings that the new approach should address. The following limitations have been the subject of numerous studies (e.g., [23,32–34]).

The main flaw is that they require an estimate of the initial distorted mound shape and assume that the interaction is between the raft and an already-distorted mound shape. Mitchell [33] has noted that one of the key factors influencing the analysis of raft foundations resting on expansive soils in all of the design methods is the initial distorted mound shape. The mound exponent, m, the maximum differential movements, y_m, and the edge moisture variation distance, e_m, determine the initial distorted mound shape. One of the main issues is thought to be determining the e_m reliably. Additionally, estimating the initial distorted mound shape has the drawback of not accounting for the soil movements that result from various edge effects, such as ponded water, tree roots, and climate.

The current design methodologies made use of three different kinds of supporting soil models, including a rigid model (1), a Winkler and coupled spring model (2), and an

elastic continuum model (3). Because of the soil's compressibility, the stiff model used by the BRAB method did not permit any decrease in the edge moisture variation distance, leading to extremely conservative structural design parameters. The soil was represented by independent springs in the Winkler model, each of which had a stiffness known as the modulus of subgrade reaction. According to Winkler's theory, the vertical displacement at a given point in the foundation is proportional to the contact pressure there. The primary limitation of the Winkler model is its inability to account for the soil's shearing resistance. The coupled spring model captures the soil's behavior in the absence of lateral displacement quite accurately. The model that best captures the behavior of the soil is thought to be the elastic continuum model [32].

The concentrated loads from columns are disregarded, and only two forms of structural loads (i.e., uniformly distributed loads and perimeter line loads) were taken into account by any of the approaches. Put another way, every design technique currently in use is appropriate for wall-bearing structures but inappropriate for use with reinforced concrete structures made up of slabs, beams, and columns.

A few of the current techniques were created for one-story residential buildings (e.g., [23]).

The majority of the design techniques currently in use ignored the third direction and instead focused on the interaction between the distorted mound shape and the stiffened raft in two dimensions. Put differently; they treat the raft similarly to a beam on an elastic foundation or a strip footing.

Pidgeon [35] advises using all of the current design methodologies with caution in areas other than their original development. The present study employs a design methodology that seeks to enhance the rationality of previous design approaches and to be suitable for the design of the stiffened raft under reinforced concrete, lightweight structures that are constructed on expansive soils in Saudi Arabia.

2.2. Computer Program SLAB97

A program named SLAB97 has been developed by the second author and his colleagues to analyze the stiffened raft–expansive soil interaction. The program is able to estimate the behavior of stiffened rafts subjected to concentrated column loads and resting on expansive soils. SLAB97 takes into account two problems that are solved separately: (1) analysis of the interactions between the stiffened raft and the 3D distorted mound shapes as a result of the soil movements and (2) 3D moisture movement (i.e., changes in soil suction) in the expansive soil underneath a flexible cover such as a raft and the associated soil movements. Since the vertical stress beneath the raft affects moisture movements in the supporting expansive soil, the analysis of these two problems actually had an impact on each other. The movements in the expansive soils beneath the stiffened raft or the outcome of the initial issue determine the structural analysis of the structure. To simplify computation, every issue is resolved independently. SLAB97 coupling between the finite element model was used to solve the second problem, and the 3D moisture diffusion and soil movements model was used to solve the first problem. A number of papers [24,36–38] have described and validated the two models. For background information, a brief description of the SLAB97 program is provided below.

The finite difference method, FDM, in the SLAB97 program, was used to solve the 3D suction diffusion equation, and the finite element method, FEM, which is based on the classical theory of thin plate on elastic half-space, was used to solve the stiffened raft–3D distorted mound shape interaction. Mitchell [39] developed the 3D suction diffusion equation, and Wray's model [40] served as the basis for the computation of soil movements, such as shrinkage or heave.

As illustrated in Figure 2, the raft and soil mass are discretized and represented as a grid of nodes. According to El-Garhy [41] and Abu Ali et al. [42], the size of the modeled soil mass beneath the stiffened raft is taken to be greater than the size of the raft by $B/4$ from each side. The advantage of symmetry can be considered in SLAB97 to spare time. In the

present study, for the solution of the 3D transient suction diffusion equation, the boundary conditions at the soil surface, outside the domain of the raft, are taken equal to $(\psi_e + \psi_0)$ and beneath the raft as well as at the end of the active zone is considered equal to ψ_e as shown in Figure 2. Whereas, at the corners of the soil mass and its sides (i.e., $x - z$ and $y - z$ planes), the boundary values of soil suction are obtained by solving the transient suction diffusion equation in 1D and 2D under the boundary conditions of $(\psi_e + \psi_0)$ at the top and ψ_e at the bottom, respectively.

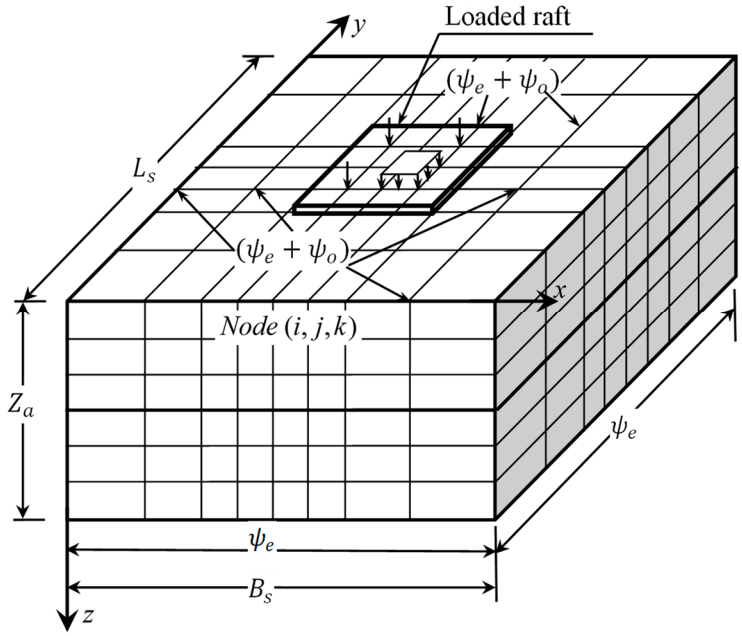

Figure 2. The discretization of the raft and the underneath soil mass for the SLAB97 program.

Some of the drawbacks of the current design methods are addressed by the program SLAB97. These include (1) predicting the response of the stiffened raft to changes in the climatic boundary conditions simply by stating the initial soil suction conditions in the soil mass; (2) taking into account the interaction between the stiffened raft and the distorted mound shape in three dimensions; (3) avoiding the need to prescribe the maximum differential movement and edge moisture variation distance as input values, as well as the locations of the points not in contact between the raft and the subgrade and the gap at these points. It does, however, necessitate estimating the worst-case scenario for the climatic boundary conditions, which could result in the worst possible distribution of soil suction throughout the expansive soil mass beneath the stiffened raft over the course of its lifetime.

SLAB97 is capable of estimating the 3D initial distorted mound shapes in addition to determining the maximum and minimum values of deflections, shears, and moments required for structural design, as well as the values induced in the stiffened raft. One of the benefits of the SLAB97 program's analysis of stiffened rafts is that it considers all of the variables that could influence the outcome, such as (1) load factors, (2) soil factors, (3) stiffened raft factors, and (4) climatic factors. The 3D initial distorted mound shape is produced by the interaction of the climatic and soil factors, and the deflections and internal forces induced in the stiffened raft are produced by the interaction of the stiffened raft and the initial distorted mound shape.

Validation of the Program SLAB97

El-Garhy et al. [36] reported the validation of the program SLAB97 against field measurements by comparing its results with the measured displacements of an actual raft resting on expansive soils at Sunshine, Melbourne, Australia. by Holland et al. [29]. In

addition to previous validation, the problem of rafts resting on expansive soil has been solved by Shams et al. [43] resolved by SLAB97, and the results are compared for the purpose of more program validation. Shams et al. (2018) solved the raft problem by two different methods (i.e., ABAQUS program and AS2870-2011 [44]) for the two cases of ES and EH. The raft is of dimensions 20 m × 20 m and rests on a 4 m expansive soil layer. The thickness of the raft is 55 cm in the case of ES and 90 cm in the case of EH. The raft is subjected to a uniformly distributed load of 6.5 kPa plus its own weight and a perimeter line load of 10 kN/m. The elasticity modulus and Poisson's ratios of the raft and the expansive soil are 2.1×10^4 MPa, 0.16 and 80 MPa, 0.30, respectively.

The SLAB97 program's input parameters are chosen to generate a mound heave value that is similar to the mound heave employed by Shams et al. [43] in order to facilitate appropriate comparison. The values of the equilibrium soil suction, the amplitude of surface suction change, the diffusion coefficient of the soil, and the suction compression index of 2.0 p^F, 4.0 p^F 0.08 m^2/day, and 0.0215, respectively, are used in the present analysis for the two cases of ES and EH. The SLAB97 program analyzes a 20 m × 20 m raft that is resting on an expansive soil mass with dimensions of 30 m × 30 m × 4 m. Only a quarter of the raft and the supporting soil mass are taken into account because of symmetry about the x and y axes.

Figures 3–6 show comparisons among the results of the SLAB97 program, ABAQUS program, and AS2870-2011 method. For the cases of ES, an excellent comparison is obtained between the distorted surface movements along the x axis of the SLAB97 program and the AS2870-2011 method, whereas the maximum differential movement of the SLAB97 program is greater than that of the ABAQUS program, as shown in Figure 3. The predicted deflection at the center of the raft by the SLAB97 program is slightly greater than the deflections predicted by the ABAQUS program and AS2870-2011 method, whereas, at the mid-edge point of the raft, the deflection of SLAB97 is equal to the deflection of the AS2870-2011 method and slightly smaller than the deflection of the ABAQUS program as shown in Figure 3. The predicted differential deflection along the x-axis by the SLAB97 program (i.e., 15.63 mm) is smaller than the differential deflections predicted by the ABAQUS program and AS2870-2011 method by about 18.4% and 53.6%, respectively. The maximum bending moment along the x-axis predicted by the SLAB97 program (i.e., 205.2 kN·m/m) is greater than that predicted by the ABAQUS program and AS2870-2011 method by about 13.3% and its location at 4 m from raft edge whereas, the location of the maximum moments of the other two methods at 5 m from the edge of the raft as shown in Figure 4.

For the case EH, the difference in the distorted surface mound shapes of the three methods is clear; however, the maximum differential movement is approximately equal, as shown in Figure 5. The predicted maximum deflection at the raft center by the SLAB97 program (i.e., 26.41 mm) is greater than the deflections predicted by the ABAQUS program and AS2870-2011 method by about 35.3% and 26.5%, respectively. However, the predicted differential deflection along the x-axis by the SLAB97 program (i.e., 16.79 mm) is slightly smaller than the differential deflection predicted by the ABAQUS program (i.e., 17.1 mm) and smaller than that predicted by the AS2870-2011 method by about 15.5% as shown in Figure 5. The maximum bending moment at the center of the raft predicted by the SLAB97 program (i.e., 578.6 kN·m/m) is slightly greater than that predicted by the ABAQUS program and AS2870-2011 method by about 11.5% and 8.96%, respectively, as shown in Figure 6.

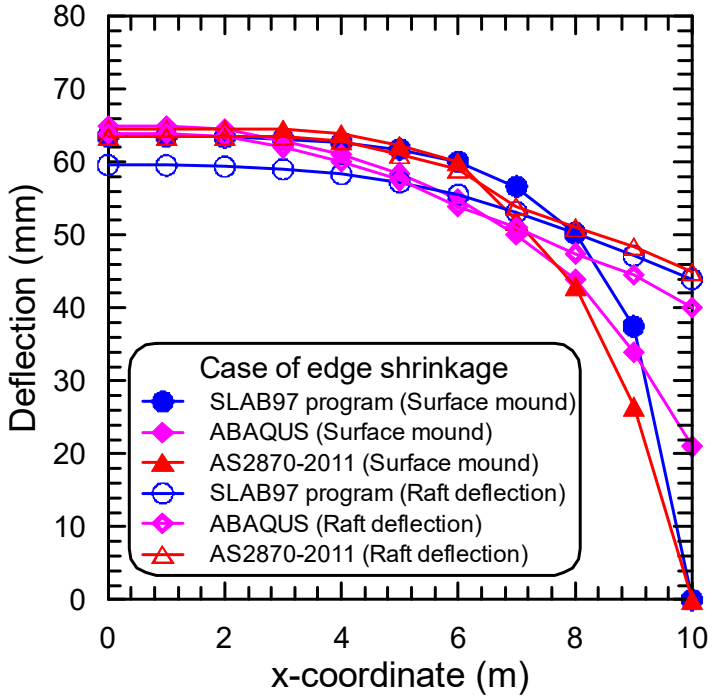

Figure 3. Comparisons between SLAB97 results and others for the surface mound shape and raft deflection (case of ES).

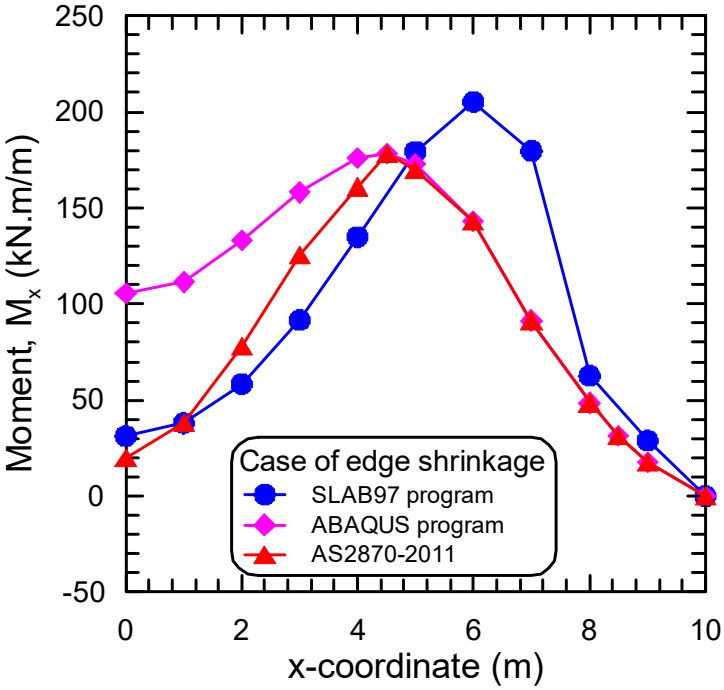

Figure 4. Comparisons between SLAB97 results and others for bending moments (case of ES).

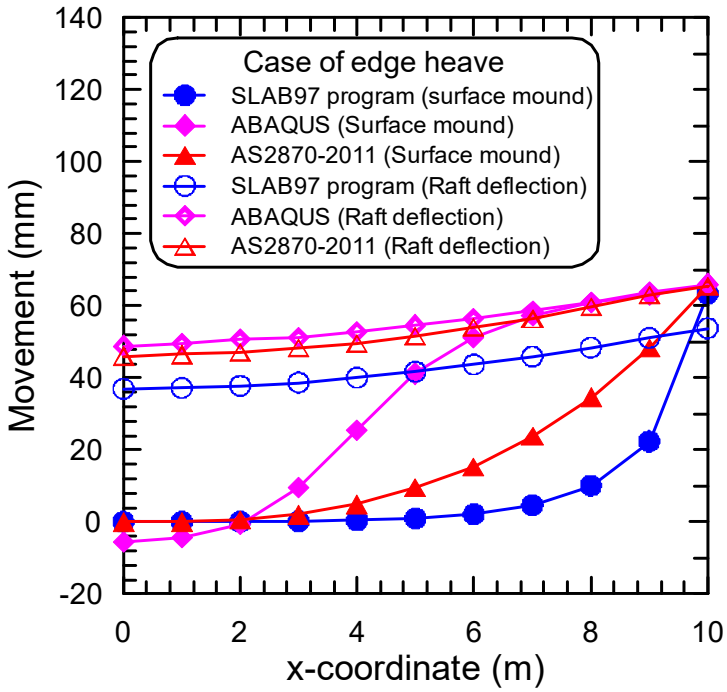

Figure 5. Comparisons between SLAB97 results and others for the surface mound shape and raft deflection (case of EH).

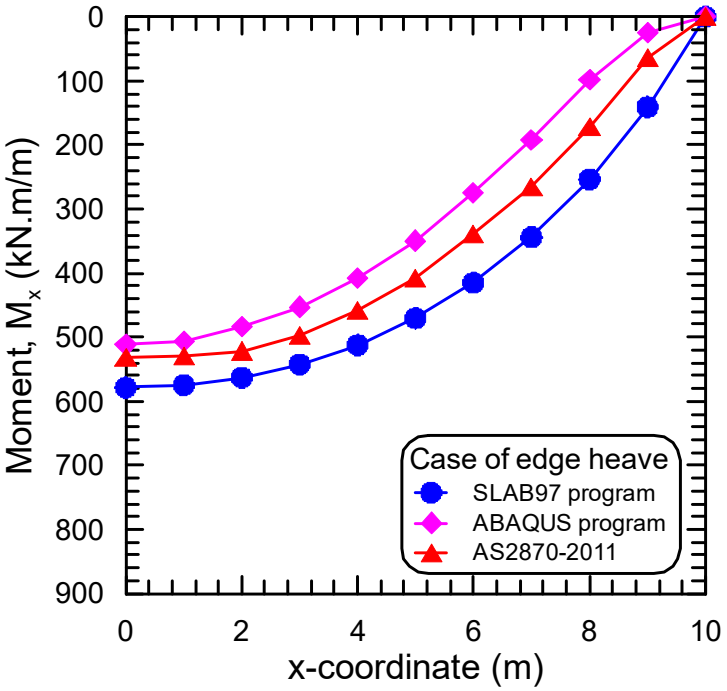

Figure 6. Comparisons between SLAB97 results and others for bending moments (case of EH).

3. Parametric Study

A parametric study is conducted using the SLAB97 program to examine the impact of different parameters on the stiffened rafts' behavior when they are built on expansive soils. These parameters are the raft's dimensions, L/B, the maximum differential movement of the mound shapes, y_m, and the depth of the stiffening beam d.

The following input parameters must be known at any site in order to use the SLAB97 program to calculate the structural design parameters (i.e., deflections, shears, and mo-

ments) of a stiffened raft resting on expansive soil: the equilibrium soil suction, ψ_e, the diffusion coefficient, α, the suction compression index, SCI, the amplitude of the surface suction change, ψ_o, and the depth of the active zone, Z_a, are the four initial parameters. Additionally, it is important to know the initial values of soil suctions in the expansive soil as well as the worst predicted weather scenarios that could result in the worst variations in soil suctions through the expansive soil beneath the raft over the course of its lifetime. Abu-Ali et al. [42] developed a rational procedure for estimating the climate-controlled soil parameters (i.e., α, ψ_o, Z_a, SCI, and ψ_o) from the results of routine geotechnical tests. They used their procedure and estimated the climate-controlled soil parameters for expansive soils at various locations in the KSA.

In this study, an equilibrium suction condition beneath the raft followed by a four-month dry spell (i.e., extended draught) to simulate the distortion mode of ES, and an equilibrium suction condition in the soil mass underneath the raft followed by a four-month wet spell (i.e., extended wet) to simulate the distortion mode of EH [3,38]. For the two instances of distortion modes with maximum differential movements, y_m, covering the soil classes taken into consideration in the Australian standard [44], it was found that a period of four months was sufficient to predict the distribution of wet and dry suction through the soil mass.

One of the climate-controlled parameters affecting the distorted mound shapes (i.e., the diffusion coefficient) is changed. In contrast, the other parameters are left unchanged to minimize the parameters affecting the analysis of the interaction between the stiffened rafts and the distorted mound shapes.

Because there are no measurements for the maximum differential movements, y_m, due to climatic changes at all locations of Saudia Arabia, and since the climatic conditions in the KSA are very close to the climatic conditions in large areas of Australia, the diffusion coefficient is changed to produce mound shapes of maximum differential movements, y_m, covering the soil classes (i.e., slightly reactive to extremely reactive) considered in the Australian standard [44]. The values of the climate-controlled parameters considered in the parametric study are selected to cover the range of those parameters in the different KSA locations, as shown in Table 1.

Table 1. Range of the parametric study's parameters.

Z_a (m)	ψ_e p^F (kPa)	ψ_o p^F (kPa)	SCI	α (m^2/Day)	Raft Size $B \times L$ (m × m)	Aspect Ratio (L/B)	Stiffening Beam Depth (m)
5.0	4.0 (1000)	2.0 (10)	0.02	0.00144 0.00432 0.0104 0.0200 0.0360	8 × 8 12 × 16 16 × 28 20 × 40	1.00 1.33 1.75 2.00	0.30 0.60 0.90 1.20 1.50

The site classes recommended by the Australian standard [44] along with the values of the y_m considered in the parametric study for different rafts are shown in Table 2. As recommended by [44], the $y_m = 0.7\ y_s$ for footing design.

The modulus of elasticity of the soil, E_s, is taken at 60 MPa and 20 MPa for ES and EH, respectively, and its Poisson ratio is 0.4. The creep modulus of elasticity and Poisson's ratio of the raft are 12,000 MPa and 0.15, respectively. The raft thickness and stiffening beams width and spacing are kept constant and equal to 0.15 m, 0.30 m, and 4 m, respectively. The stiffening beam depth varies and includes the slab thickness.

The most common type of construction in the KSA is reinforced concrete structures, which consist of slabs, beams, columns, and footings. This study concerns the lightweight-reinforced concrete structures (e.g., Villas) consisting of three stories, which are usually susceptible to expansive soil problems. Unlike most of the previous studies, two types of

loads are considered in the present study. These are column loads and a uniform distributed load representing the weight of the raft, the flooring, and the live loads.

Table 2. Site classes according to [44], along with the y_m values considered in the parametric study.

Site Classes According to AS2870-2011 [44]			Values of the y_m Considered in the Parametric Study (mm)			
Class	Site classification	y_s (mm)	Raft size (m × m)			
			8 × 8	12 × 16	16 × 28	20 × 40
S	Slightly reactive	$0 < y_s \leq 20$	20.14	20.52	20.52	20.52
M	Moderately reactive	$20 < y_s \leq 40$	31.37	32.88	32.88	32.88
H1	Highly reactive	$40 < y_s \leq 60$	45.60	48.52	48.52	48.51
H2	Highly reactive	$60 < y_s \leq 75$	58.54	63.68	63.76	63.75
E	Extremely reactive	$y_s > 75$	67.92	76.77	77.32	77.37

The columns' loads are calculated by the approximate tributary area method [45] based on an equivalent uniform load (i.e., dead load and live load) for each story = 11.63 kN/m^2. Figure 7 shows the dimensions of the studied stiffened rafts along with the columns' loads, columns dimensions, and spacing of stiffening beams.

The equivalent moment of inertia, I_{eq}, is used in the SLAB97 program to calculate the equivalent rigidity of the stiffened raft.

$$I_{eq} = \sqrt{I_x^2 + I_y^2} \tag{1}$$

where I_x and I_y are the moments of inertia per unit width of stiffened raft cross-section in x and y directions

To determine the equivalent thickness of the raft, the equivalent rigidity is equated to the rigidity of the constant raft thickness as follows.

$$h_{eq} = \sqrt[3]{12(1 - v_r^2) I_{eq}} \tag{2}$$

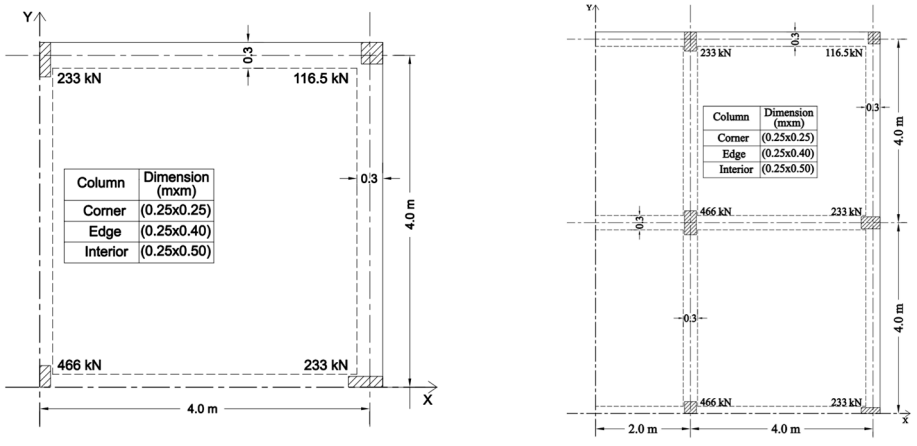

(**a**) (**b**)

Figure 7. *Cont.*

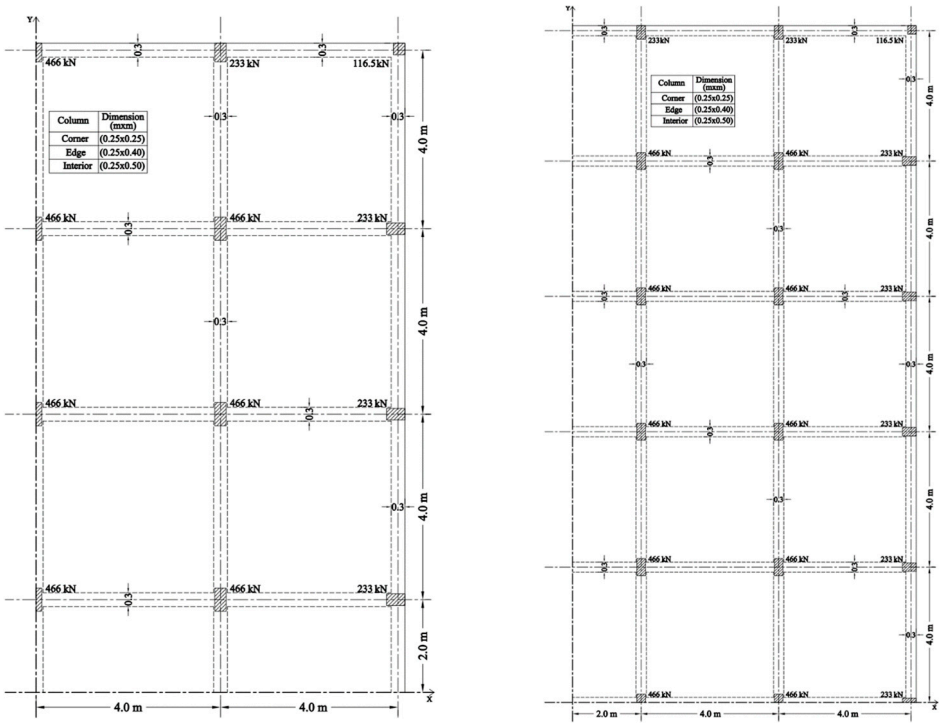

Figure 7. Dimensions and loads of the studied rafts: (**a**) raft size 8 m × 8 m, (**b**) raft size 12 m × 16 m, (**c**) raft size 16 m × 28 m, (**d**) raft size 20 m × 40 m.

4. Analysis of Results

The obtained results from the parametric study are used to investigate the effect of stiffening beam depth, the maximum differential movement of mound shape, and the raft dimensions represented by the aspect ratio, L/B, on the distribution of deflections and bending moments along the x and y axes. For space limitations, only the results of rafts of sizes 8 m × 8 m and 16 m × 28 m are presented here.

4.1. Effect of the Stiffening Beam Depth

The effect of the stiffening beam depth on the distribution of deflections and bending moments induced in the stiffened raft along the x and y axes for the rafts (i.e., 8 m × 8 m and 16 m × 28 m) at the maximum y_m shown in Table 2 (i.e., 67.92 mm and 77.32 mm) for two distortion modes of ES and EH are presented and discussed in this section.

For the case of ES, Figures 8–11 show the effect of beam depth on the deflections, bending moments, and the initial surface movements along the x and y axes for rafts of sizes 8 m × 8 m and 16 m × 28 m. As illustrated in these Figures, it is observed that: (1) The total and differential deflections (differential deflection is the difference between the deflections at the center of the raft and the mid-edge points on the x or y axes) decrease as the beam depth increases, (2) the length of the unsupported raft, L_{ur} (i.e., the distance inward from the edge of the raft to the point of separation between soil and raft) decreases as the beam depth increases in the x and y axes because of an increase in the raft deflections as a result of decreasing the beam depth (e.g., at the beam depths of 0.6, 0.9, and 1.2 m, the lengths of the unsupported raft are 0.80, 0.92, and 1.2 m for raft size 8 m × 8 m as shown in Figure 8 whereas, those lengths are 0.0, 0.88, and 0.96 m in the x direction and 0.84, 0.98, and 1.06 m in the y direction for raft size 16 m × 28 m as shown in Figure 10), (3) The distance from the edge of the raft to the point of separation between soil and raft, L_{ur}, is smaller than the distance from the edge of the raft to the point of the maximum moment in the two directions (e.g., at the beam depths of 0.6, 0.9, and 1.2 m, the lengths of L_{ur} are 0.84, 0.98, and 1.06 m for raft size 16 m × 28 min the y direction whereas the distance to the points of

maximum moments are 2.0, 2.3, and 5.0 m, respectively, as shown in Figure 11). A similar observation has been reported by Briaud et al. (2016) from the analysis of a stiffened raft on expansive soil subjected to uniform and perimeter line loads using ABAQUS software and they referred to the reason as that overhanging raft (i.e., raft on a dome shape mound) does not behave as a pure cantilever, (4) The distance from the raft edge to the points of maximum moments in the two directions increases as the beam depth increases (e.g., at beam depths of 0.6, 0.9, and 1.2 m, the distances to the points of maximum moments are 2.5, 3.0, and 3.5 m in x and y directions for raft size 8 m × 8 m as shown in Figure 9 and for raft size 16 m × 28 m the distances to the points of maximum moments are 1.0, 2.0, and 3.0 m in x direction and 3.0, 3.3, and 4.0 m in the y direction and as shown Figure 11), and (5) the bending moments induced in all stiffened rafts are negative moments because of the dome shape of the distorted mound and the bending moments along the x or y axes are not taken the same trends in some cases as shown in Figures 9 and 11 and this is may be due to the difference in the final contact area between the stiffened rafts and the distorted mound of expansive soils in the two directions and the columns concentrated loads.

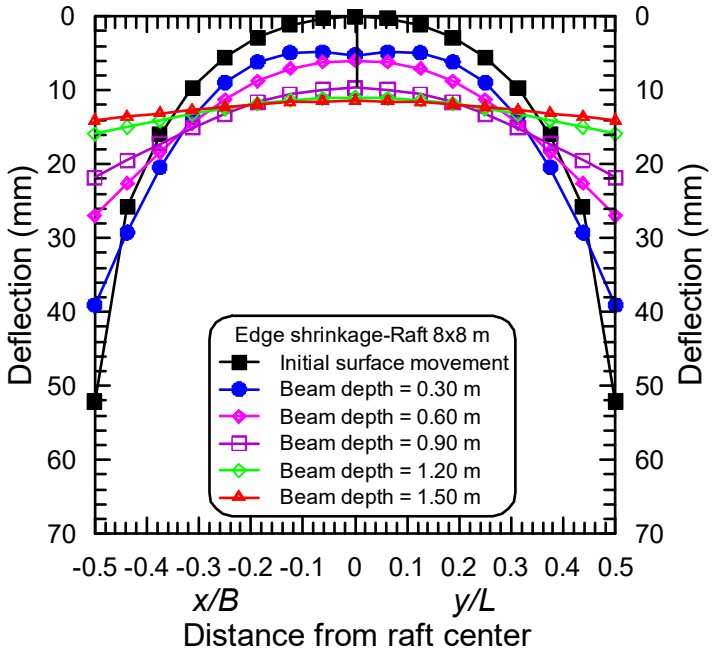

Figure 8. Effect of beam depth on the deflection along with the initial surface movement through the x and y axes for raft size 8 m × 8 m (case of ES).

For the case of EH, Figures 12–15 show the effect of beam depth on the distribution of deflections and bending moments along the x and y axes for rafts of sizes 8 m × 8 m and 16 m × 28 m. Referring to these Figures, it is shown that (1) generally, total and differential deflections decrease as the beam depth increases, and (2) two types of soil supports are observed; these are simply support conditions and multiple support conditions. For raft size 8 m × 8 m at beam depths of 0.6, 0.9, 1.2, and 1.5 m simply support occurs, and the raft behaves as a slab supported at its edges whereas, at beam depth of 0.3 m, multiple supports (i.e., support at the raft perimeter and support at the raft core area) are occurred as shown in Figure 12. For raft size 16 m × 28 m full contact occurs between the raft and soil in the x direction for all beam depths, whereas, in the y direction, full contact occurs except for cases of beam depths of 1.2 m and 1.5 m as shown in Figure 14. This explains the difference in the trends of the bending moments along the x or y axes, as shown in Figures 13 and 15. The two types of soil supports are observed by Shams et al. [23] from the analysis of stiffened rafts of single-story building subjected to a uniform load and a perimeter line load using ABAQUS software, (3) for raft size 8 m × 8 m because of the simple soil support condition, at beam depths of 0.6, 0.9, 1.2, and 1.5 m, the maximum moments occurred at the center

of the raft and the moments taken the same trends except for the beam depth of 0.3 m the moments shows a different trend because of multiple soil support condition as shown in Figure 12 while, for raft size 16 m × 28 m, at all beam depths, the maximum moments occurred near the raft edges and shows similar trends in both x and y direction as shown in Figure 15 and this is attributable to the full contact between the rafts and soil, at all beam depths, because of the heavy interior columns loads, (4) for raft size 16 m × 28 m, the distance inward from raft edge to the point of maximum moment along the x or y axes increases as the beam depth increases as shown in Figure 15, (5) the moments induced in the rafts are positive moments due to the dish shape of the distorted mound.

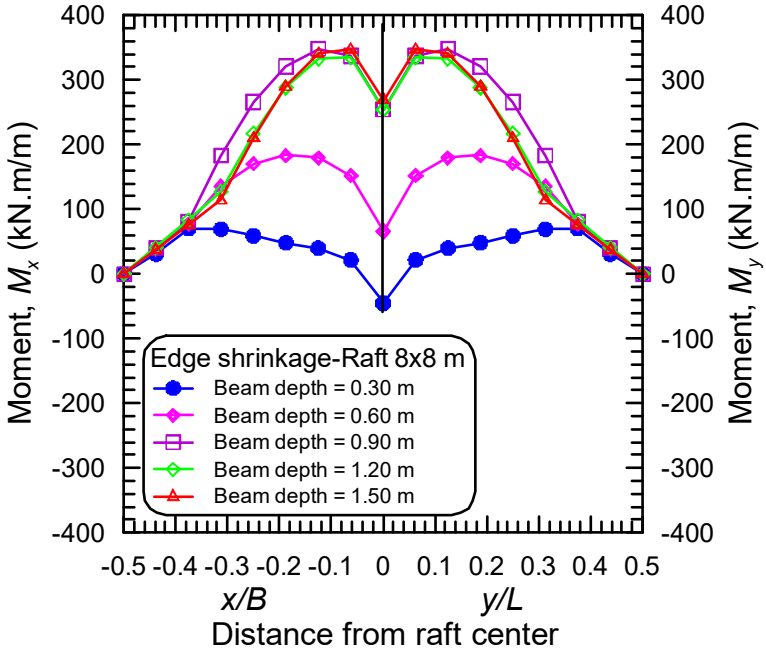

Figure 9. Effect of beam depth on the M_x and M_y through the x and y axes for raft size 8 m × 8 m (case of ES).

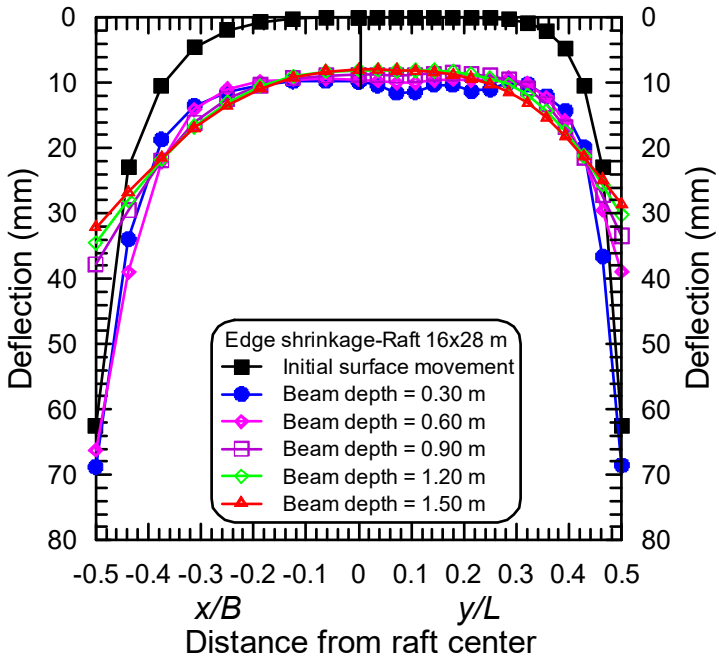

Figure 10. Effect of beam depth on the deflection along with the initial surface movement through the x and y axes for raft size 16 m × 28 m (case of ES).

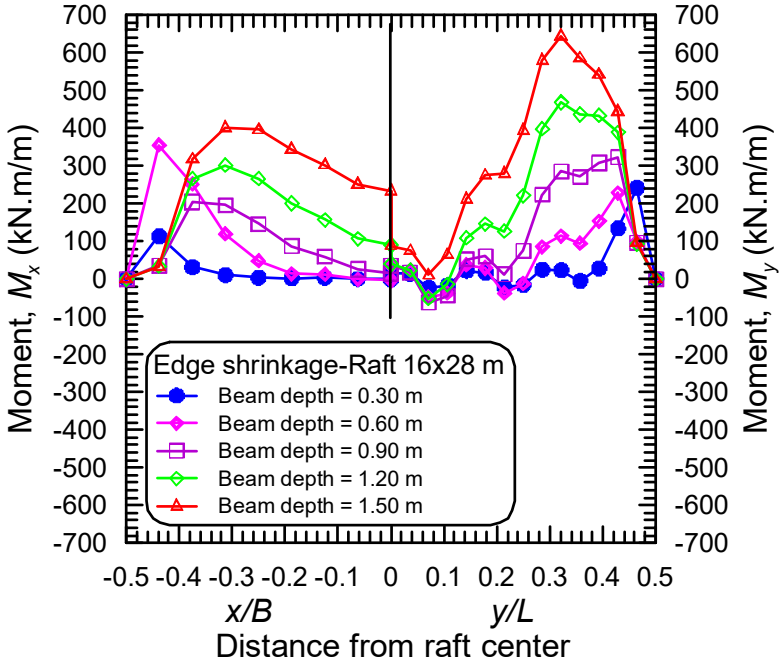

Figure 11. Effect of beam depth on the M_x and M_y through the x and y axes for raft size 16 m × 28 m (case of ES).

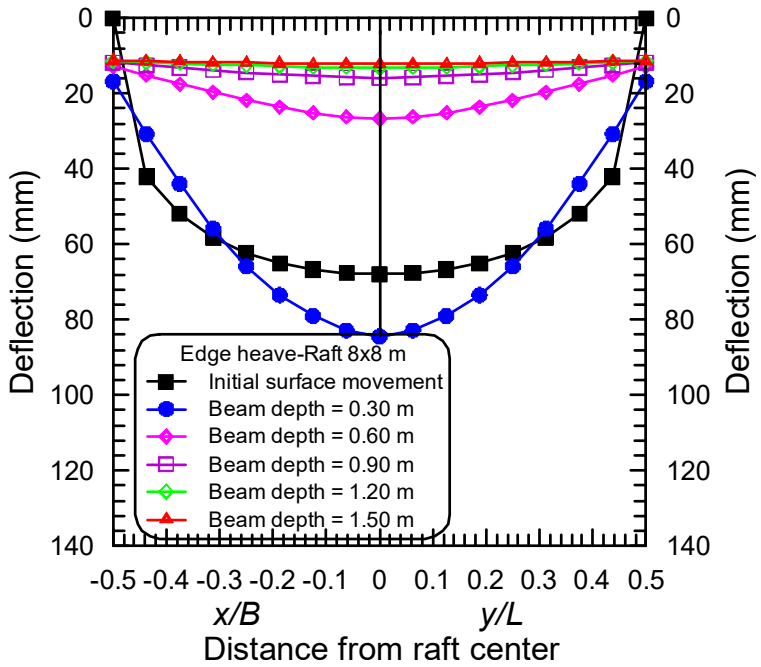

Figure 12. Effect of beam depth on the deflection along with the initial surface movement through the x and y axes for raft size 8 m × 8 m (case of EH).

The absolute values of maximum deflections and maximum bending moments along the x and y axes for the case of EH are greater than those in the case of ES for all the studied rafts except for raft size 8 m × 8 m, and this is attributable to two reasons: (1) the soil stiffness in case of EH is smaller than that in case of ES (i.e., E_s = 20 MPa in case of EH and equal to 60 MPa in case of ES) and (2) there is one interior column in case of raft size 8 m × 8 m and the rest of the columns on the raft perimeter that supported on the soil in the case of EH.

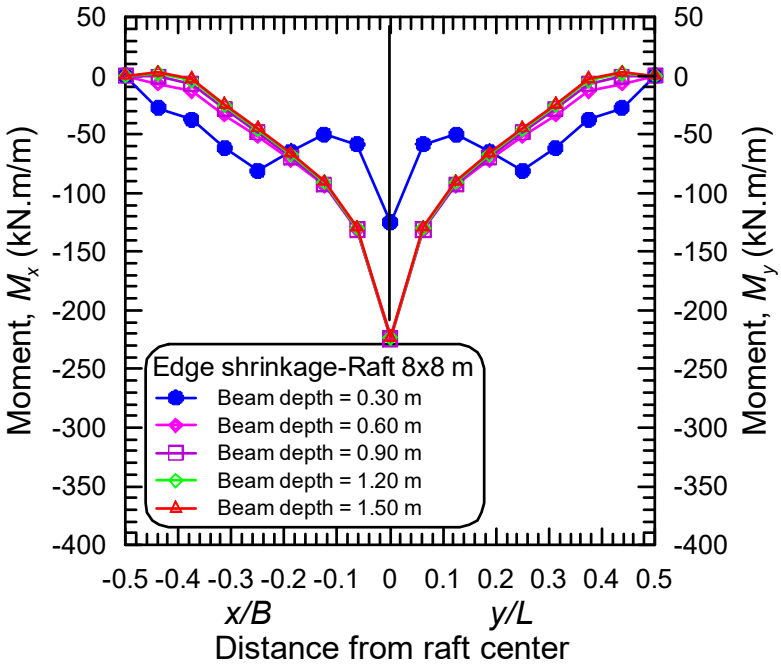

Figure 13. Effect of beam depth on the M_x and M_y through the x and y axes for raft size 8 m × 8 m (case of EH).

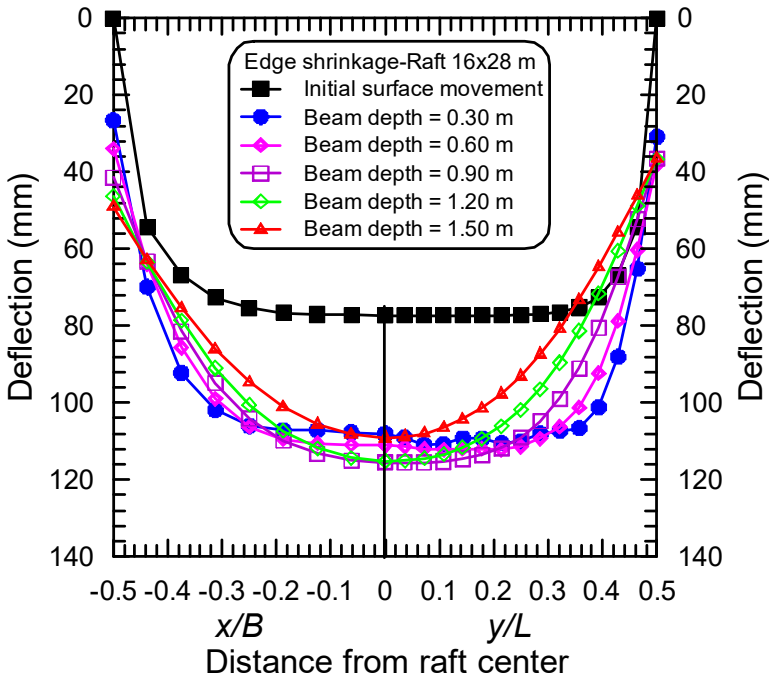

Figure 14. Effect of beam depth on the deflection along with the initial surface movement through the x and y axes for raft size 16 m × 28 m (case of EH).

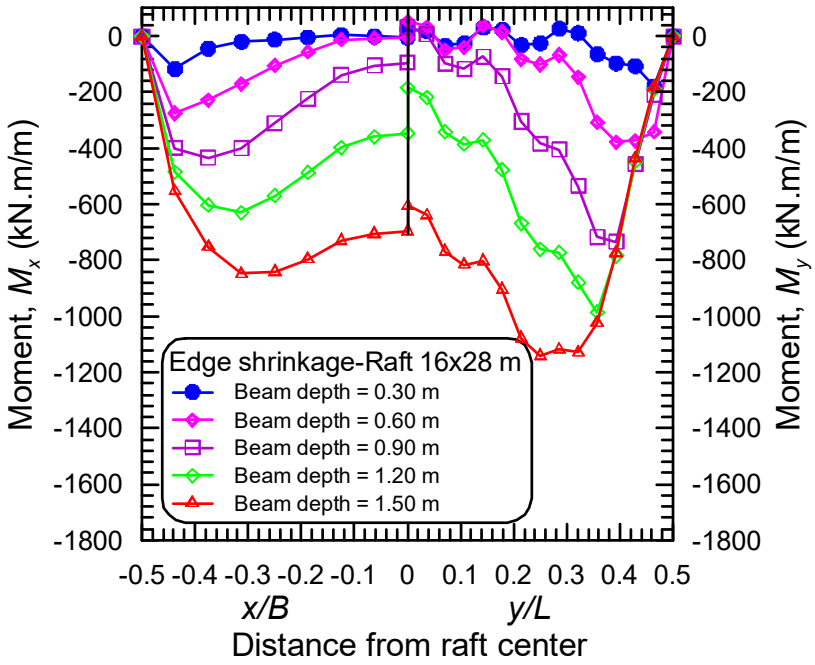

Figure 15. Effect of beam depth on the M_x and M_y through the x and y axes for raft size 16 m × 28 m (case of EH).

4.2. Effect of the Differential Movement of Mound Shape

The effect of the differential movements of mound shape, y_m, on the deflections and bending moments induced in the stiffened raft along the x and y axes, rafts of sizes 8 m × 8 m and 16 m × 28 m at beam depth of 1.2 m are presented and discussed.

For the case of ES, Figures 16–19 show the effect of the y_m on the deflections and bending moments along the x and y axes for rafts of sizes 8 m × 8 m and 16 m × 28 m. The deflections, differential deflections, and bending moments along the x and y axes increase as the y_m increases as shown in Figures 16–19, except for raft size 8 m × 8 m, the maximum differential deflections along the x and y axes at y_m = 58.54 mm is slightly greater than that at y_m = 67.92 mm by about 11.45%, and therefore, the maximum bending moments along the x and y axes at y_m = 58.54 mm is slightly greater than the maximum bending moments at y_m = 67.92 mm by about 7.7%, and this may be attributable to the maximum number of iterations (i.e., 10) considered by the program to achieve convergence, in other words, at y_m = 67.92 mm, the convergence condition may need iterations greater than 10, and this is considered a rare case. Also, from a loading point of view, a raft of size 8 m × 8 m is considered a special case because the columns' loads located on the perimeter of the raft represent 66.7% of building loads, and the load of the interior column represents 33.3% of the building loads unlike raft of size 16 m × 28 m the interior columns' loads represent 64.3% from the building loads and the columns' loads located on the perimeter of the raft represent a 35.7%. The distance inward from the raft edge to the point of maximum bending moment increases as the y_m increases as shown in Figures 17 and 19 (e.g., for raft size 8 m × 8 m, the distances from the raft edge to the points of maximum bending moments at the values of the y_m = 37.37 mm and 58.54 mm are 2.5 m and 3.0 m, respectively, and for raft size 16 m × 28 m, these distances along the y axis are 2.0 m and 5.0 m at the values of the y_m = 32.88 mm and 63.76 mm, respectively).

For the case of EH, Figures 20–23 show the effect of the y_m on the deflections and bending moments along the x and y axes for rafts of sizes 8 m × 8 m and 16 m × 28 m. For raft size 8 m × 8 m, the deflections, differential deflections, and bending moments along the x and y axes are the same at all values of the y_m as shown in Figures 20 and 21, and this is because the raft behaves as a simply supported plate at all values of the y_m because of three reasons: the high stiffness of the raft as the beam depth was 120 mm, the shortened length

of the raft, and all the column loads located on the perimeter of the raft except one interior column load acting at the raft center. Whereas, for raft size 16 m × 28 m, the deflections, differential deflections, and bending moments along the x and y axes increase as the y_m increases, as shown in Figures 22 and 23. The distance inward from the raft edge to the point of maximum bending moment along the x and y axes are the same and equal to 2.0 m for all values of y_m except for the value of y_m = 76.33 mm. This distance along the y axis was increased to 2.5 m as shown in Figure 23.

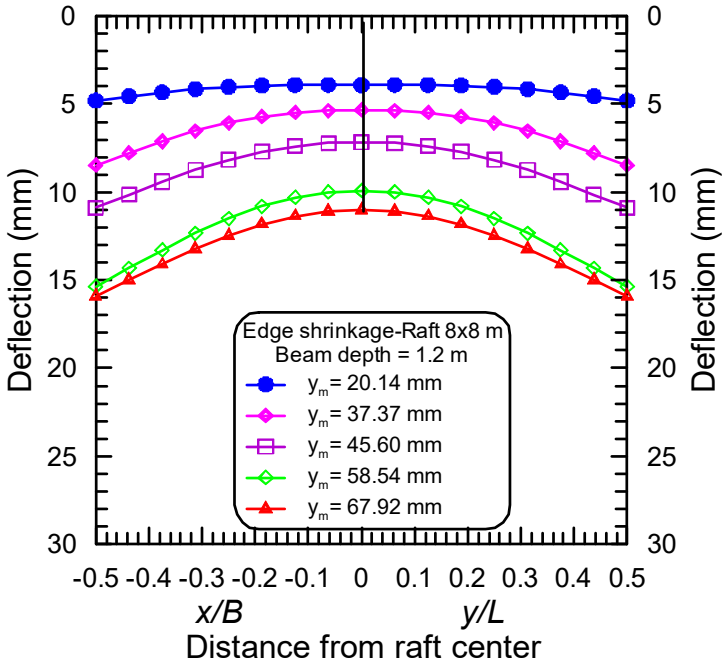

Figure 16. Effect of differential movement on the deflection through the x and y axes for raft size 8 m × 8 m (case of ES).

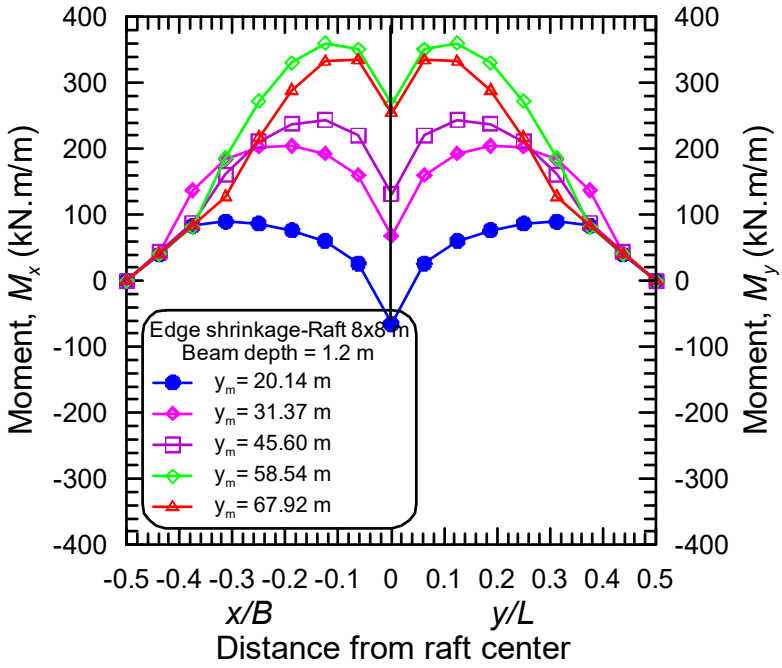

Figure 17. Effect of differential movement on the bending moments through the x and y axes for raft size 8 m × 8 m (case of ES).

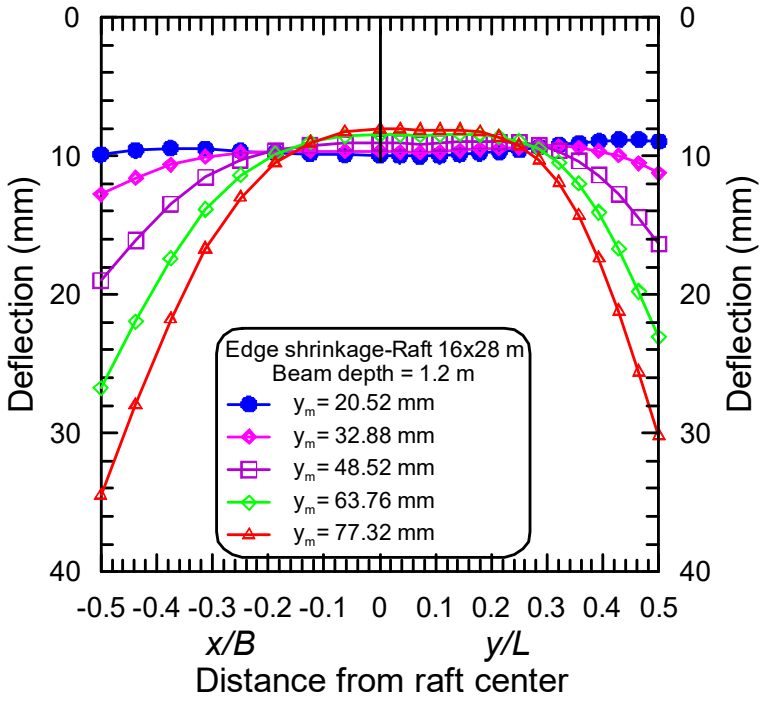

Figure 18. Effect of differential movement on the deflection through the x and y axes for raft size 16 m × 28 m (case of ES).

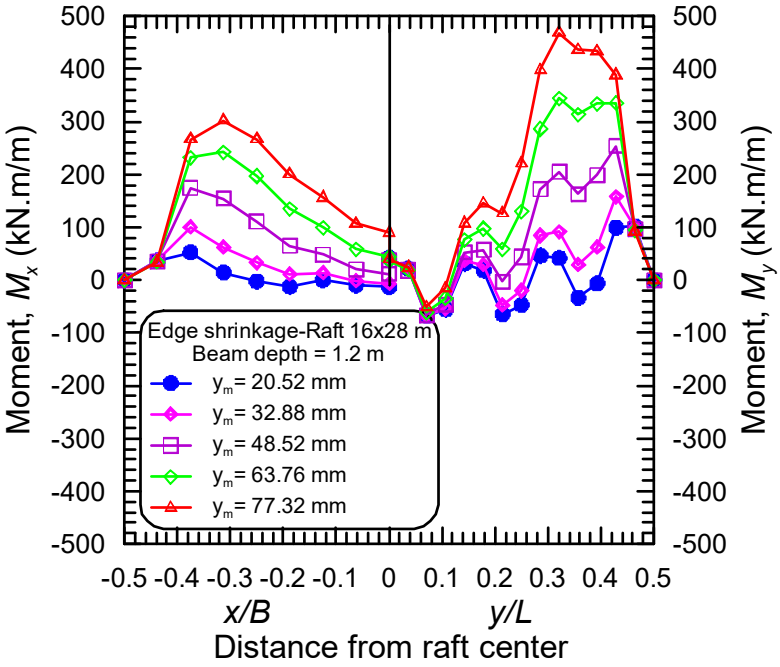

Figure 19. Effect of differential movement on the bending moments through the x and y axes for raft size 16 m × 28 m (case of ES).

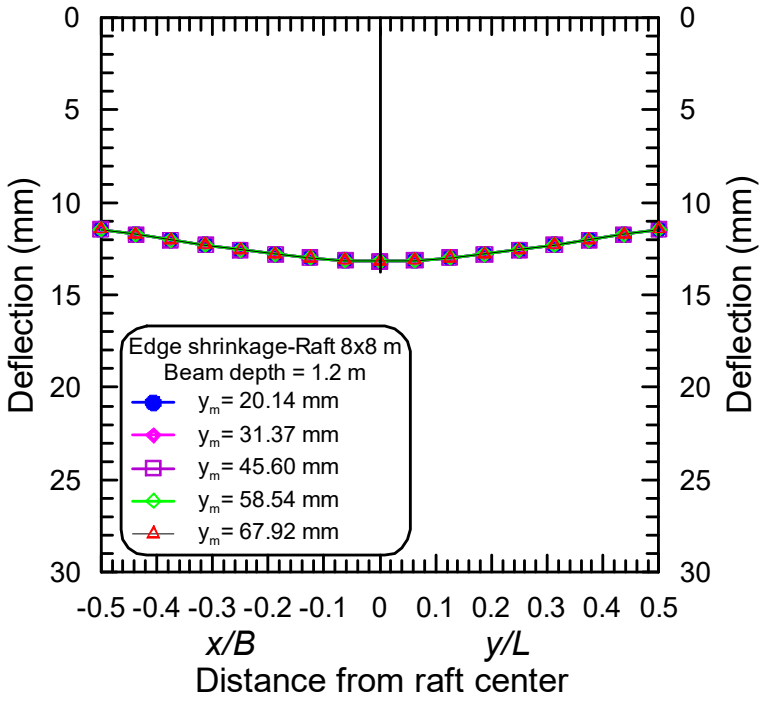

Figure 20. Effect of differential movement on the deflection through the x and y axes for raft size 8 m × 8 m (case of EH).

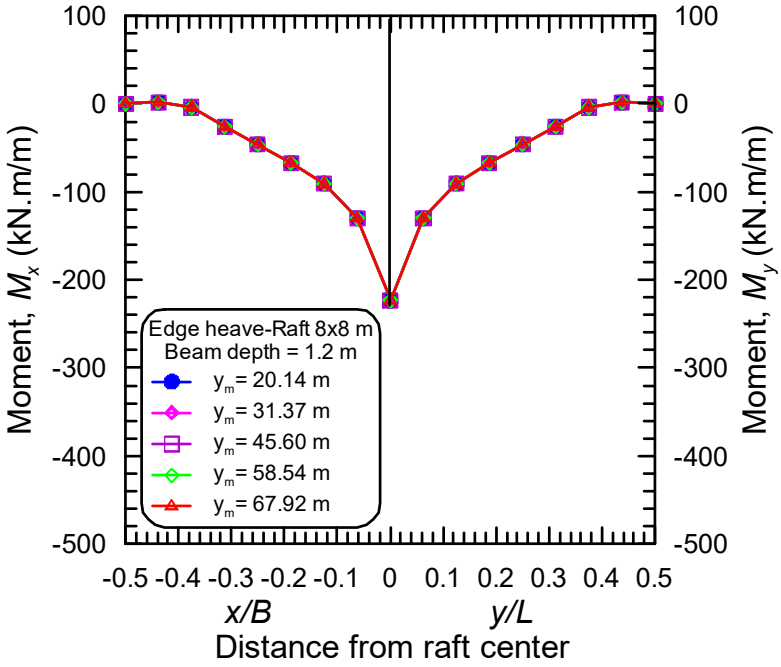

Figure 21. Effect of differential movement on the bending moments through the x and y axes for raft size 8 m × 8 m (case of EH).

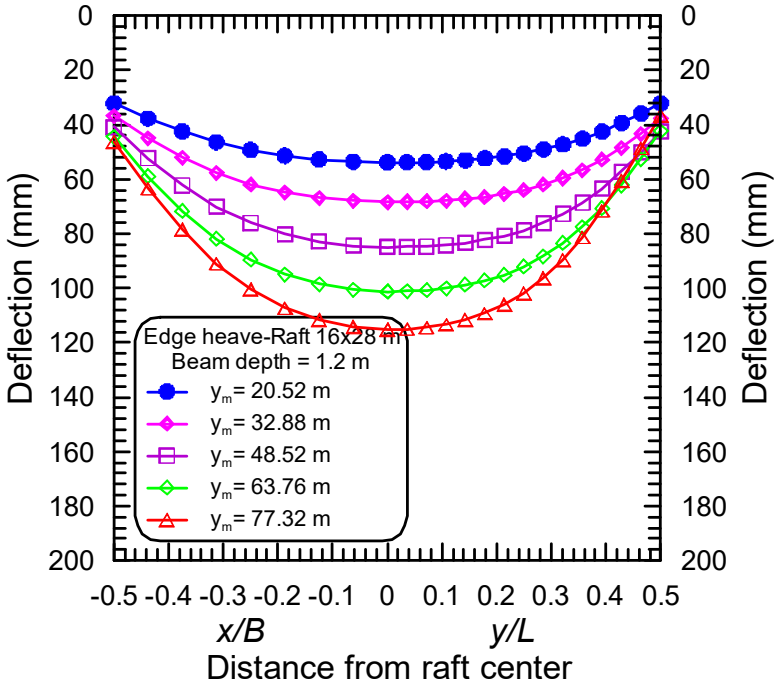

Figure 22. Effect of differential movement on the deflection through the x and y axes for raft size 16 m × 28 m (case of EH).

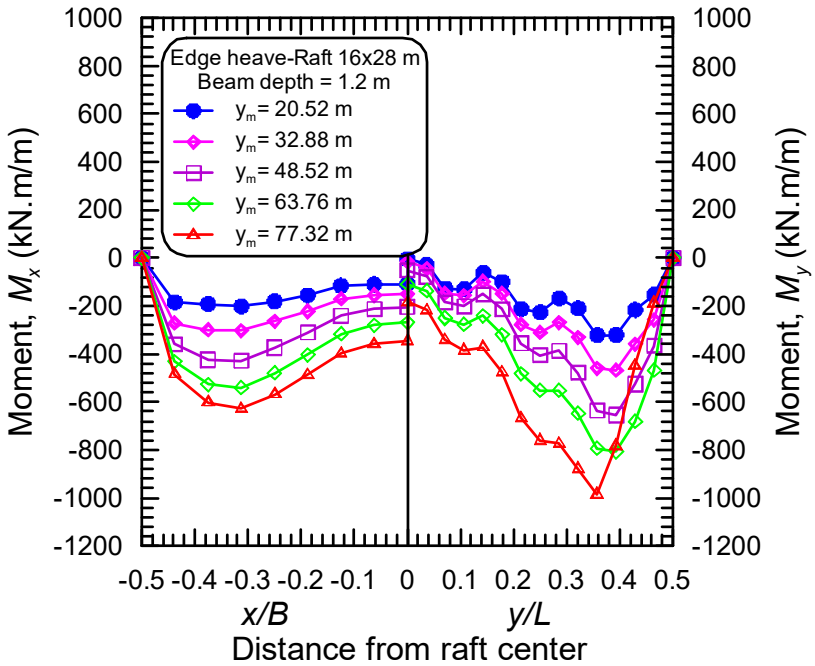

Figure 23. Effect of differential movement on the bending moments through the x and y axes for raft size 16 m × 28 m (case of EH).

4.3. Effect of Raft Dimensions

Figures 24–27 show the effect of raft dimension represented by the aspect ratio, L/B, on the deflections and bending moments induced in the raft along the x and y axes for all studied rafts at a diffusion coefficient of 0.036 m^2/day and stiffening beam depth of 1.2 m for the two cases of ES and EH. The deflections and maximum deflection along the x and y axes increase as the L/B ratio increases for the two cases of ES and EH, as shown in Figures 24 and 26. For the case of ES, the maximum bending moments

along the x and y axes increase as the L/B ratio increases, as shown in Figure 25. The distance from the raft edge to the point of maximum moments that occurred along the x and y axes decreases as the L/B ratio increases for the two cases of ES and EH, as shown in Figures 25 and 27.

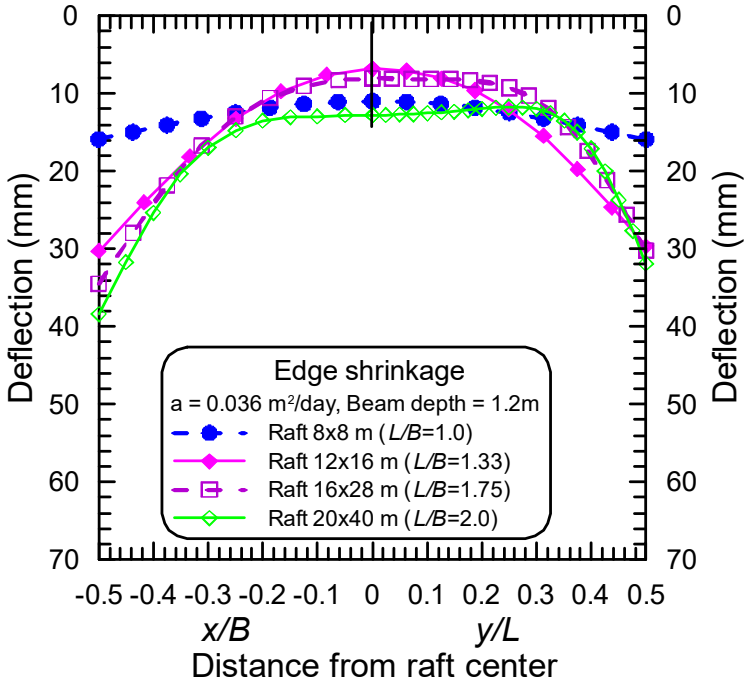

Figure 24. Effect of raft dimensions on the deflections through the x and y axes (case of ES).

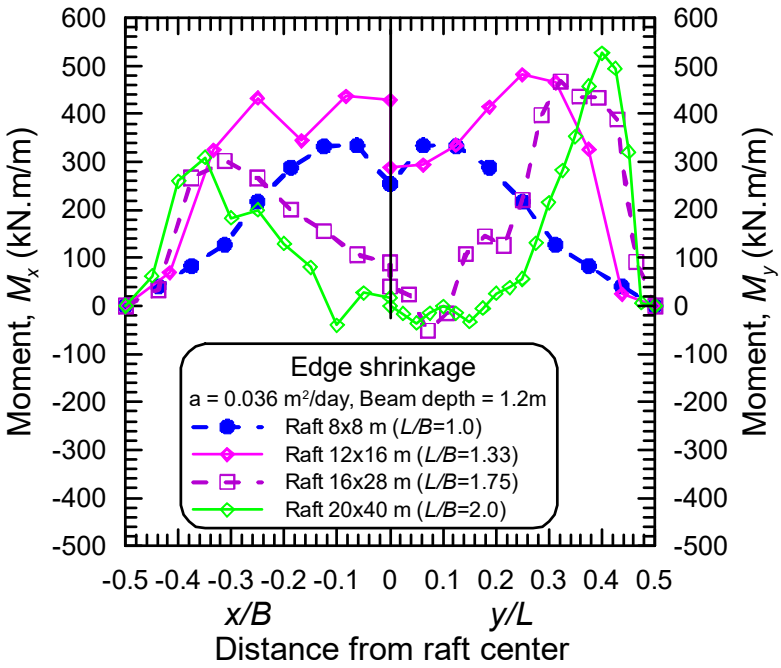

Figure 25. Effect of raft dimensions on the bending moments through the x and y axes (case of ES).

Not shown in this paper but discovered in the overall analysis is that for the studied rafts (i.e., 12 m × 16 m and 20 m × 40 m), the distribution of deflections and bending moments along the x and y axes are similar to that of raft size 16 m × 28 m with some small differences according to the condition of soil supports, the columns' loads, and the raft dimensions of each raft in both cases of ES and EH.

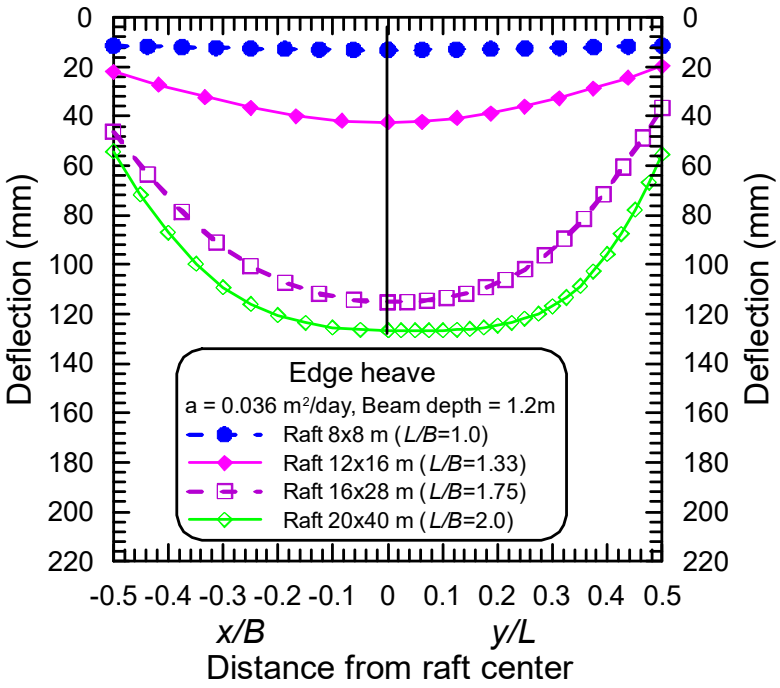

Figure 26. Effect of raft dimensions on the deflections through the x and y axes (case of EH).

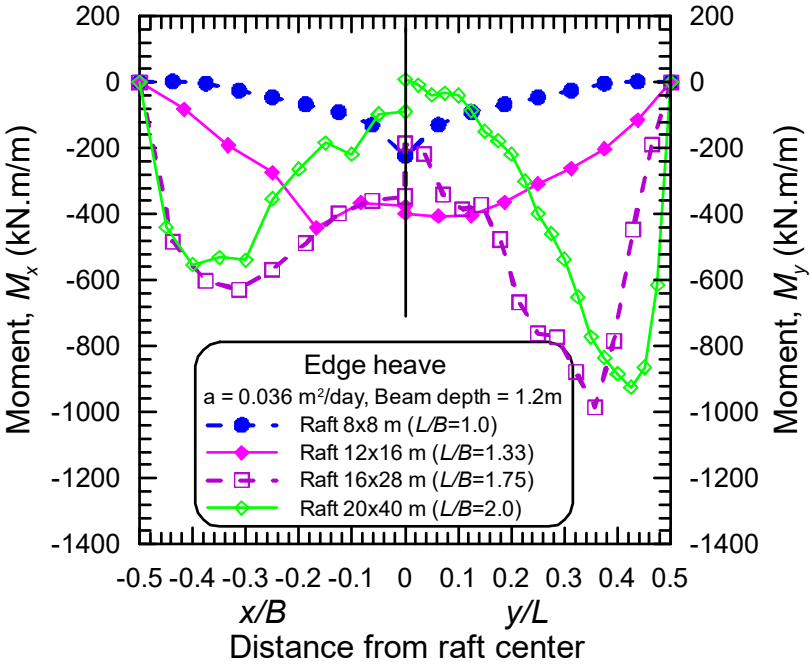

Figure 27. Effect of raft dimensions on the bending moments through the x and y axes (case of EH).

5. Conclusions

The behavior of stiffened rafts subjected to concentrated column loads and resting on expansive soils is calculated using a finite element program named SLAB97. The program can calculate the 3D distorted mound shape and examine how the stiffened raft interacts with the 3D distorted mound shape. The goal of the analysis technique presented in this work is to increase the earlier researchers' soil–raft interaction models' rationality. For both edge shrinkage and edge heave scenarios, the worst initial 3D distorted mound shapes are assumed to yield an upper-bound solution. The program has been validated by comparing its results with the results of others and shows good agreement. A parametric

investigation is carried out by the program to study the impact of different parameters (i.e., the stiffening beam depth, the maximum differential movement of the mound shape, and the raft dimensions) on the behavior of stiffened rafts resting on expansive soils for the two cases of edge shrinkage and edge heave.

The following are some of the conclusions from this study:

1. The stiffened rafts subjected to concentrated columns' loads exhibit a similar shape of raft deformation and distribution of bending moments to those of the stiffened rafts subjected to uniform and perimeter line loads in both cases of distortion modes; however, the values of the design parameters (i.e., maximum deflection, maximum differential deflection, and maximum bending moments) are completely different.
2. For the case of EH distortion mode, two conditions of soil support were observed; these are simply-support condition and multiple-supports condition (i.e., support at the raft perimeter and support at the raft core area), depending on the stiffness of the raft.
3. The maximum bending moments in long and short directions, in both distortion modes, occur near the raft edge, and the distance from the raft edge to the locations of maximum moments depends on the stiffening beam depth, the maximum differential movement, and the aspect ratio of the raft.
4. The greatest amount of differential deflection was found to occur at the corner of the raft, and its value is dependent on the stiffening beam depth, the maximum differential movement, and the raft dimensions.
5. The stiffened raft components should be designed to withstand both negative moments and positive moments arising from both two distortion modes of ES and EH, respectively.

Author Contributions: Conceptualization, M.H.A.-A.; software, B.E.-G.; validation, B.E.-G., A.B. and W.S.A.; formal analysis, B.E.-G. and A.B.; investigation, B.E.-G. and A.B.; resources, B.E.-G. and W.S.A.; data curation, B.E.-G., A.B. and H.A.-D.; writing—original draft preparation, B.E.-G., W.S.A., A.B. and B.A.; writing—review and editing, B.E.-G., A.B. and W.S.A.; visualization, M.E.-S.; supervision, M.H.A.-A.; project administration, B.E.-G.; funding acquisition, M.H.A.-A. All authors have read and agreed to the published version of the manuscript.

Funding: This research was funded by the University of Tabuk (UT), Deanship of Scientific Research, under Grant No. S-1443-0090.

Data Availability Statement: The raw data supporting the conclusions of this article will be made available by the authors on request.

Acknowledgments: This research is supported by the University of Tabuk (UT), Deanship of Scientific Research, under Grant No. S-1443-0090. The author gratefully acknowledges this financial support.

Conflicts of Interest: The authors declare no conflicts of interest.

References

1. Li, J.; Cameron, D.A.; Ren, G. Case Study and Back Analysis of a Residential Building Damaged by Expansive Soils. *Comput. Geotech.* **2014**, *56*, 89–99. [CrossRef]
2. Nelson, J.D.; Chao, K.C.; Overton, D.D.; Nelson, E.J. *Foundation Engineering for Expansive Soils*; John Wiley & Sons, Inc.: Hoboken, NJ, USA, 2015.
3. Wray, W.K. *So Your Home Is Built on Expansive Soils: A Discussion of How Expansive Soils Affect Buildings*; American Society of Civil Engineers: Reston, VA, USA, 1995.
4. Krohn, J.P.; Slosson, J.E. Assessment of expansive soils in the United States. In Proceedings of the 4th International Conference on Expansive Soils, ASCE, Denver, CO, USA, 16–18 June 1980; pp. 596–608.
5. Robert, L.; Andrew, B.; Mary, L.C. *Soils Shrink, Trees Drink, and Houses Crack*; ECOS Magazine; The Science Communication Unit of CSIRO's Bureau of Scientific Services: Adelaide, Australia, 1980; pp. 13–15.
6. Dafalla, M.A.; Al-Shamrani, M.A.; Al-Mahbashi, A. Expansive soils foundation practice in a semiarid region. *J. Perform. Constr. Facil.* **2017**, *31*, 04017084. [CrossRef]
7. Fredlund, D.G.; Rahardjo, H. *Soil Mechanics for Unsaturated Soils*; Wiley: New York, NY, USA, 1993.

8. Fredlund, D.G. The Implementation of Unsaturated Soil Mechanics into Geotechnical Engineering. *Can. Geotech. J.* **2000**, *37*, 963–986. [CrossRef]
9. Erol, O.A.; Dhowian, A.W. Swell and shrinkage behavior of Madinish active clays. *J. Eng. Sci.* **1982**, 1–8.
10. Dhowian, A.W.; Ruwaih, I.A.; Erol, A.O. The distribution and evaluation of the expansive soils in Saudi Arabia. In Proceedings of the Second Saudi Engineers Conference, Dhahran, Saudi Arabia, 17–19 November 1985; Volume 1, pp. 308–326.
11. Ruwaih, I.A. Experiences with Expansive Soils in Saudi Arabia. In Proceedings of the 6th International Conference on Expansive Soils, New Delhi, India, 1–4 December 1987; pp. 317–322.
12. Abduljauwad, S.N.; Al-Sulaimani, G.J.; Al-Buraim, I.; Basunbul, I.A. Laboratory and field studies of response of structures to heave of expansive clay. *Géotechnique* **1998**, *48*, 103–121. [CrossRef]
13. Slater, D.E. Potential Expansive Soils in Arabian Peninsula. American Society for Civil Engineering. *Geotherm. Eng.* **1983**, *109*, 744–746.
14. Abduljauwad, S.N.; Ahmed, R. Expansive Soil in Al-Qatif Area. *Arab. J. Sci. Eng.* **1990**, *15*, 133–144.
15. Dhowian, A.W.; Erol, A.O.; Youssef, A. *Evaluation of Expansive Soils and Foundation Methodology in the Kingdom of Saudi Arabia*; General Directorate Research Grants Programs, King Abdulaziz City for Science and Technology: Riyadh, Saudi Arabia, 1990.
16. Abduljauwad, S.N. Swelling Behavior of Calcareous Clays from the Eastern Province of Saudi Arabia. *J. Eng. Geol.* **1994**, *27*, 333–351.
17. Al-Refeai, T.; Al-Ghamdy, D. Geological and geotechnical aspects of Saudi Arabia. *Geotech. Geol. Eng.* **1994**, *12*, 253–276. [CrossRef]
18. Dafalla, M.; Al-Shamrani, M. *Geocharacteristics of Tabuk Expansive Shale and Its Links to Structural Damage*; Geo-Congress 2014 Technical Papers; American Society of Civil Engineers: Reston, VA, USA, 2014; pp. 882–889.
19. Sabtan, A.A. Geotechnical Properties of Expansive Clay Shale in Tabuk, Saudi Arabia. *J. Asian Earth Sci.* **2005**, *25*, 747–757. [CrossRef]
20. Dafalla, M.A.; Al-Shamrani, M.A. "Performance-Based Solutions for Foundations on expansive Soils-Al Ghatt Region", Saudi Arabia. In Proceedings of the International Conference on Geotechnical Engineering, Chiangmai, Thailand, 10–12 December 2008.
21. Dafalla, M.A.; Al-Shamrani, M.A. Expansive Soil Properties in a Semi-Arid Region. *Res. J. Environ. Earth Sci.* **2012**, *4*, 930–938.
22. Dafalla, M.A.; Al-Shamrani, M.A.; Puppala, A.; Ali, H.E. *Use of Rigid Foundation System on Expansive Soils*; GSP (Geotechnical Special Publication); American Society for Civil Engineers (ASCE): Reston, VA, USA, 2010; p. 199.
23. Shams, M.A.; Shahin, M.A.; Ismail, M.A. Design of stiffened slab foundations on reactive soils using 3D numerical modeling. *Int. J. Geomech.* **2020**, *20*, 04020097. [CrossRef]
24. Wray, W.K.; El-Garhy, B.M.; Youssef, A.A. Three-Dimensional Model for Moisture and Volume Changes Prediction in Expansive Soils. American Society of Civil Engineering, ASCE. *J. Geotech. Geoenviron. Eng.* **2005**, *131*, 311–324. [CrossRef]
25. Briaud, J.L.; Abdelmalak, R.; Zhang, X.; Magbo, C. Stiffened slab-on-grade on shrink-swell soil: New design method. *J. Geotech. Geoenviron. Eng.* **2016**, *142*, 04016017. [CrossRef]
26. Building Research Advisory Board (BRAB). *Criteria for Selection and Design of Residential Slabs-on-Ground*; National Research Council, Academy of Sciences, Publication 1571; Building Research Advisory Board (BRAB): Washington, DC, USA, 1968.
27. Lytton, H. Observation Studies of Parent-Child Interaction, A Methodological Review. *Child Dev.* **1971**, *42*, 651–684. [CrossRef]
28. Walsh, D.S. *Papers in Pidgin and Creole Linguistics No. 1. (Pacific Linguistics A-54)*; Australian National University Press: Canberra, Australia, 1978; pp. 185–197.
29. Holland, J.E.; Pitt, W.G.; Lawrance, C.E.; Cimino, D.J. The Behavior and Design of Housing Slabs on Expansive Soils. In Proceedings of the Fourth International Conference on Expansive Soils, Denver, CO, USA, 16–18 June 1980; Volume 1, pp. 448–468.
30. Mitchell, P. A Simple method of design of shallow footings on expansive soil. In Proceedings of the 5th International Conference on Expansive Soils, Adelaide, SA, USA, 21–23 May 1984.
31. Post-Tensioning Institute (PTI). *Design and Construction of Post-Tensioned Slabs-on-Ground*, 2nd ed.; Post-Tensioning Institute: Phoenix, AZ, USA, 1996.
32. Wray, W.K. Development of a Design Procedure for Residential and Light Commercial Slabs-on-Ground Constructed over Expansive Soils. Ph.D. Dissertation, Texas A&M University, College Station, TX, USA, 1978.
33. Mitchell, P.W. The Design of Footings on Expansive Soils. Engineering Problems of Regional Soils. In Proceedings of the International Conference, Beijing, China, 8–12 August 1988; pp. 127–135.
34. Teodosio, B.; Baduge, K.S.K.; Pmendis, P. A review and comparison of design methods for raft substructures on expansive soils. *J. Build. Eng.* **2021**, *41*, 102737. [CrossRef]
35. Pidgeon, J.D. A Comparison of the suitability of two soils for direct drilling of spring barley. *Eur. J. Soil Sci.* **1980**, *31*, 581–594. [CrossRef]
36. El-Garhy, B.M.; Wray, W.K.; Youssef, A.A. Using Soil Diffusion to Design Raft Foundation on Expansive Soils. In Proceedings of the Sessions of Geo-Denver, Denver, CO, USA, 3–8 August 2000; Geotechnical Special Publication No. 99. ASCE: Reston, VA, USA, 2000; pp. 586–602.
37. El-Garhy, B.M.; Youssef, A.A.; Wray, W.K. Predicted and Measured Suction and Volume Changes in Expansive Soil. In Proceedings of the International Symposium on Suction, Swelling, Permeability and Structure of Clays, Shizuoka, Japan, 11–13 January 2001.
38. El-Garhy, B.M.; Wray, W.K. Method for Calculating the Edge Moisture Variation Distance. *J. Geotech. Geoenviron. Eng.* **2004**, *130*, 945–955. [CrossRef]

39. Mitchell, P.W. *The Structural Analysis of Footings on Expansive Soil*; Research Report No. I; Kenneth W. G. Smith and Associates: Adelaide, Australia, 1979.
40. Wray, W.K. *Using Soil Suction to Estimate Differential Soil Shrink or Heave*; Unsaturated Soil Engineering Practice, Geotechnical Special Publication No. 68; American Society of Civil Engineers: Reston, VA, USA, 1997; pp. 66–87.
41. E1-Garhy, B.M. Soil Suction and Analysis of Raft Foundation Resting on Expansive Soils. Ph.D. Dissertation, Civil Engineering Department, Menoufia University, Shebin EI-Koon, Egypt, 1999.
42. Abu-Ali, M.H.; El-Garhy, B.; Boraey, A.; Al-Rashed, W.S.; Abdel-Daiem, H. Estimating the Climate-Controlled Soil Parameters and the Distorted Mound Shape for Analysis of Stiffened Rafts on Expansive Soils. *Adv. Civ. Eng.* **2024**, *2024*, 5599356. [CrossRef]
43. Shams, M.A.; Shahin, M.A.; Ismail, M.A. Analysis and Modelling of Stiffened Slab Foundation on Expansive Soils. In *Numerical Analysis of Nonlinear Coupled Problems, GeoMEast 2017, Sustainable Civil Infrastructures*; Shehata, H., Rashed, Y., Eds.; Springer: Cham, Switzerland, 2018. [CrossRef]
44. *AS2870-2011*; Residential Slabs and Footings. Australian Standards: Sydney, NSW, Australia, 2011.
45. Hibbeler, R.C. *Structural Analysis*, 7th ed.; Prentice Hall: Saddle River, NJ, USA, 2011.